Dicle University
Journal of Engineering
https://dergipark.org.tr/tr/pub/dumf
duje.dicle.edu.tr

Research Article

# Convergence studies for static analysis of thin plates on Pasternak Foundations

**Ülkü Hülya ÇALIK-KARAKÖSE***

Istanbul Technical University, Civil Engineering Department, calikkarakose@itu.edu.tr, Orcid No: 0000-0002-2944-7434

ARTICLE INFO

*Article history*:

Received 2 January 2023
Received in revised form 8 March 2023
Accepted 9 March 2023
Available online 23 March 2023

*Keywords:*

*Kirchhoff plate element, Reissner-Mindlin plate element, Pasternak foundation, shear locking, convergence*

*Doi: 10.24012/dumf.1228192*

* Corresponding author

ABSTRACT

Convergence studies for the static analysis of thin plates resting on Pasternak foundations is performed. The plates are discretized using two different finite elements, the formulations of which are based on the Kirchhoff and Reissner-Mindlin plate theories. The shear locking problem which arises when full integration is used in the finite element implementation of Reissner-Mindlin plate theory is eliminated with selective integration. The Pasternak foundation is accounted for by adding the parameter matrices of an existing soil finite element to the stiffness matrix terms of the plate finite elements corresponding to deflections. Convergence rates for different boundary conditions, plate thicknesses and soil parameters are obtained and given comparatively through numerical examples.

## Introduction

Bending analyses of plates are performed using the differential equations of appropriate plate theories. The well-known Kirchhoff plate theory (Kirchhoff PT) which is used in the analysis of thin plates and where the shear deformation effects are neglected is developed by Love [1] following the assumptions given by Kirchhoff [2]. According to the theory, the thickness of the plate does not change and straight lines orthogonal to the midplane of the undeformed plate remain straight and orthogonal after deformation and $C^1$ continuous elements are required in the finite element implementation. The Reissner-Mindlin plate theory (R-M PT) [3,4] which is mostly used for the analysis of thick plates can also be used for the analysis of thin plates. In this theory, shear deformation and rotary inertia effects are taken into consideration and straight lines orthogonal to the midplane of the plate remain straight but not orthogonal to the midplane after deformation. In the finite element implementation, $C^0$ continuous elements suffice.

Shear locking problem arises when R-M plate elements are used in the analysis of thin plates which is due to the excessive effect of the transverse shear deformation terms in the formulations. This problem can be alleviated using several techniques like reduced or selective integration, non-conforming element method, assumed shear strain method, the discrete shear gap method, or the mixed interpolation of tensorial components method. In this paper, selective integration technique is utilized to eliminate the shear locking problem as done in [5].

The simplest model used for the analysis of plates resting on elastic foundations is the Winkler (one-parameter) model [6] where the interaction between the plate and the foundation is accounted for using independent linear elastic springs. In this model, shear interaction between the springs does not exist which leads to deflection discontinuity on the plate surface. This deficiency is avoided in Pasternak (two-parameter) model [7] where the shear interaction between the springs is defined via a second parameter. Static analyses of isotropic rectangular plates resting on Pasternak foundation are performed in many studies as in [8-9]. A semi-analytical solution for the static analysis of thin skew plates on Winkler and Pasternak foundations is presented by [10]. In a recent study, a computing method for bending analysis of thin plates resting on Pasternak foundation is developed, [11]. Vibration analyses of isotropic rectangular plates resting on Pasternak foundation are also performed in many studies, [12-14].

In this study, a MATLAB code is written for the convergence studies on static analysis of thin plates resting on Pasternak foundations using [15]. The plates are discretized using two different finite elements which are based on Kirchhoff and R-M plate theories. The Kirchhoff plate finite element is a popular four-noded twelve degree of freedom (DOF) rectangular plate element developed by [16] and [17,18] (also known as MZC plate element) and the R-M plate finite element is a bilinear four-noded twelve DOF quadrilateral plate element developed by [19,20].

Elastic bedding and shear parameter matrices of a soil finite element which are derived by [9] are added to the corresponding terms of the plate stiffness matrices to account for the Pasternak foundation. Midpoint deflections and convergence rates of thin plates discretized using Kirchhoff plate elements and R-M plate elements with full integration and selective integration, are obtained for different plate thicknesses, foundation parameters and boundary conditions.

## Kirchhoff Plate Element

The thin plate bending finite element, the formulation of which is based on Kirchhoff plate theory is a four-noded rectangular finite element having three DOFs (one deflection and two rotations) at each node, Figure 1.

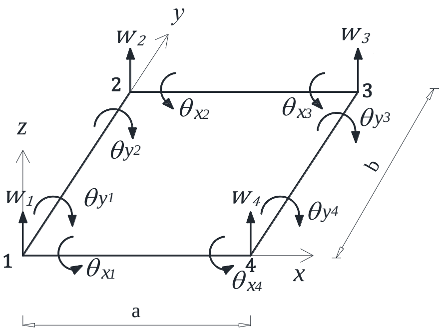


Figure 1. Plate finite element

The displacement vector of the finite element is

$$u = \{w \quad \theta_x \quad \theta_y\}^T \tag{1}$$

where the rotations are expressed in terms of deflections as

$$\theta_x = \frac{\partial w}{\partial y} \quad , \quad \theta_y = -\frac{\partial w}{\partial x} \tag{2}$$

The stress-strain relation of classical elasticity is

$$[\sigma_b] = [C_b][\varepsilon] \tag{3}$$

where the strain vector is

$$[\varepsilon] = \begin{Bmatrix} -\dfrac{\partial^2 w}{\partial x^2} \\ -\dfrac{\partial^2 w}{\partial y^2} \\ -2\dfrac{\partial^2 w}{\partial x \partial y} \end{Bmatrix} \tag{4}$$

and the material matrix for the isotropic material is defined as

$$[C_b] = \frac{Eh^3}{12(1-\nu^2)} \begin{bmatrix} 1 & \nu & 0 \\ \nu & 1 & 0 \\ 0 & 0 & \dfrac{1-\nu}{2} \end{bmatrix} \tag{5}$$

where E is the modulus of elasticity, $h$ is the thickness of the plate and $\nu$ is the Poisson's ratio. The displacement function of the twelve DOF finite element consists of incomplete 3rd order polynomials only satisfying the deflection compatibility.

The continuum displacements $u$ are obtained by solving the fourth-order partial differential equation (p.d.e.)

$$L^T C_b L u + b = 0 \tag{6}$$

where $L$ is the derivative operator given as

$$[L] = \begin{Bmatrix} -\dfrac{\partial^2}{\partial x^2} \\ -\dfrac{\partial^2}{\partial y^2} \\ -2\dfrac{\partial^2}{\partial x \partial y} \end{Bmatrix} \tag{7}$$

and $b$ are the body forces. In the finite element discretization, the continuum displacements $u$ are expressed in terms of nodal displacements $\underline{u}$ as $u = N_k \underline{u}$ where $N_k$ are C[1] continuous shape functions used to obtain the unknown nodal displacements. The discretization gives

$$\int_A B^T C_b B dA \, \underline{u} = K\underline{u} = F \tag{8}$$

where $K$ is the element stiffness matrix, $B = LN_k$ and $F$ is the element nodal external force vector.

## Reissner-Mindlin Plate Element

The Reissner-Mindlin plate finite element is a four-noded quadrilateral element having the same DOFs, Figure 1. The displacement components of the element are

$$w \quad , \quad \theta_x = \frac{\partial w}{\partial y} + \varphi_y \; , \quad \theta_y = \frac{\partial w}{\partial x} + \varphi_x \tag{9}$$

where additional rotations ($\varphi_y$ and $\varphi_x$) arise due to the shear deformation effects. Thus, the rotations $\theta_x$ and $\theta_y$ depend on both deflection and additional rotations and they are taken as independent variables.

For bending and shear, the stress-strain relations of classical elasticity are

$$[\sigma_b] = [C_b][\varepsilon_b] \quad , \quad [\sigma_s] = [C_s][\varepsilon_s] \tag{10}$$

and the isotropic material matrix for shear is

$$[C_s] = \frac{kEh}{2(1+\upsilon)} \begin{bmatrix} 1 & 0 \\ 0 & 1 \end{bmatrix} \tag{11}$$

where $k$ is the shear correction factor. Strains for bending and shear are

$$\varepsilon_b = L_b u \quad , \quad \varepsilon_s = L_s u \tag{12}$$

respectively where the derivative operators are defined as

$$[L_b] = \begin{bmatrix} 0 & \dfrac{\partial}{\partial x} & 0 \\ 0 & 0 & \dfrac{\partial}{\partial y} \\ 0 & \dfrac{\partial}{\partial y} & \dfrac{\partial}{\partial x} \end{bmatrix} \quad , \quad [L_s] = \begin{bmatrix} \dfrac{\partial}{\partial x} & -1 & 0 \\ \dfrac{\partial}{\partial y} & 0 & -1 \end{bmatrix} \tag{13}$$

The finite element discretization gives

$$\int_A (B_b^T C_b B_b + B_s^T C_s B_s) dA\, \underline{u} = K\underline{u} = F \qquad (14)$$

where, $B_b = L_b N_i$ , $B_s = L_s N_i$ and $\underline{u}$ indicates the nodal displacement components.

Note that $C^0$ continuous bilinear shape functions $(N_i)$ are used for all of the nodal unknowns in the finite element discretization and the two stiffness matrix components in Eq. (14) are for bending and shear, respectively.

## Idealization of the Pasternak Foundation

The Pasternak foundation under the Kirchhoff and Reissner-Mindlin plates is represented by the inclusion of elastic bedding and shear parameter matrices of a soil finite element derived by [9] in the plate finite element stiffness matrices. The elastic bedding and shear parameter matrix terms $C_{ij}$ and $C_{T\,ij}$ are obtained via

$$C_{ij} = k_w \int_A w_i w_j dA \qquad (15)$$

$$C_{T\,ij} = k_p \int_A \frac{\partial w_i}{\partial x}\frac{\partial w_j}{\partial x} + \frac{\partial w_i}{\partial y}\frac{\partial w_j}{\partial y} dA \qquad (16)$$

where $k_w$ and $k_p$ respectively indicate the coefficient of subgrade reaction and the shear modulus of the foundation. The elastic bedding and shear parameter matrices $[C]$ and $[C_T]$ are obtained as

$$[C] = \frac{k_w ab}{36}\begin{bmatrix} 4 & 2 & 2 & 1 \\ 2 & 4 & 1 & 2 \\ 2 & 1 & 4 & 2 \\ 1 & 2 & 2 & 4 \end{bmatrix} \qquad (17)$$

and

$$[C_T] = \frac{k_p}{3}\begin{bmatrix} \alpha+\beta & \alpha/2-\beta & \beta/2-\alpha & -(\alpha+\beta)/2 \\ \alpha/2-\beta & \alpha+\beta & -(\alpha+\beta)/2 & \beta/2-\alpha \\ \beta/2-\alpha & -(\alpha+\beta)/2 & \alpha+\beta & \alpha/2-\beta \\ -(\alpha+\beta)/2 & \beta/2-\alpha & \alpha/2-\beta & \alpha+\beta \end{bmatrix} \qquad (18)$$

Here, $\alpha = a/b$ and $\beta = b/a$ where $a$ and $b$ are the plate dimensions.

These matrix terms are added to the stiffness matrix terms of the Kirchhoff and R-M plate elements which correspond to deflections. In [21], this procedure is carried out for the Kirchhoff plate element only.

Thus, the resulting system of equations is

$$K\underline{u} + C\underline{u} + C_T\underline{u} = F \qquad (19)$$

## Numerical Examples

### Verification Example

In order to verify the present model, a simply supported square plate resting on a Pasternak foundation subjected to a uniformly distributed load of $q=E/10^5$ kN/m$^2$ is solved for different foundation parameters using Kirchhoff and R-M plate finite elements and dimensionless midpoint deflections are compared with those in [22] as given in Table 1. A schematic representation of the plate-foundation system is given in Figure 2 noting that the system is created with plate finite elements only, since the properties of the foundation are embedded in the plate stiffness matrix.

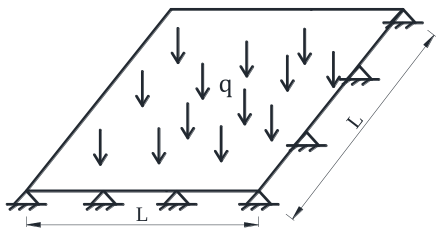


Figure 2. Simply supported square plate-foundation system

Thickness to length ratio (*h/L*) of the plate is 1/100 and υ=0.3. $k_w$' and $k_p$' are dimensionless soil parameters which are defined as $k_w' = k_w L^4 / D$ and $k_p' = k_p L^2 / D$ where $D = \frac{Eh^3}{12(1-\upsilon^2)}$. It is seen that the deflections obtained using Kirchhoff plate finite elements and R-M plate finite elements with selective integration (2x2 and 1x1 gauss points for bending and shear stiffness matrices, respectively) are very close to the reference values. It is also observed that the dimensionless deflection values decrease as the shear modulus of the foundation increases.

Table 1. Dimensionless midpoint deflections of the simply supported square plate on Pasternak foundation

| $k_w$' | $k_p$' | Dimensionless midpoint deflection ($w' = 10^3 D\, w / qL^4$) | | |
|---|---|---|---|---|
| | | Kirchhoff PT | R-M PT (sel.int.) | [22] |
| 1 | 1 | 3.8517 | 3.8855 | 3.8530 |
| 1 | $3^4$ | 0.7637 | 0.7647 | 0.7630 |
| 1 | $5^4$ | 0.1154 | 0.1154 | 0.1150 |

**Simply supported square plate on Pasternak foundation**

A simply supported square plate resting on an isotropic Pasternak foundation is solved for different plate thicknesses and foundation parameters. The plate is subjected to a uniformly distributed load $q$=1 kN/m$^2$. The plate length is L=1 m, the modulus of elasticity is E=1x10$^8$ kN/m$^2$ and the Poisson's ratio is υ =0.3.

The finite element implementation of the plate-foundation system is carried out both using Kirchhoff and R-M plate finite elements for two different thickness to length ratios (1/50 and 1/100) as well as for successively refined meshes ((4x4), (8x8), (16x16), (32x32), (64x64)). Comparisons are made for the dimensionless midpoint deflections and for the convergence rates which are obtained via L2 norm displacement error analysis.

The relative displacement errors are obtained using

$$\|e\|_2 = \frac{\|u_e - u_c\|}{\|u_e\|} = \sqrt{\frac{\int_A (u_e - u_c)^2 dA}{\int_A (u_e)^2 dA}} \qquad (20)$$

which is in L2 norm. Here, $u_c$ indicate the calculated values of the displacements, $u_e$ are the exact displacements obtained using an overkill mesh (64x64) and $A$ is the plate domain.

In the finite element implementation using Kirchhoff plate elements, (2x2) gauss integration points suffice according to the gauss quadrature rule since the displacement function of the element is an incomplete third order polynomial. In the implementation using R-M plate elements, two different gauss quadrature rules are utilized, full integration with (2x2) gauss points both for bending and shear stiffness matrices and selective integration with (2x2) gauss points for the bending stiffness matrix and a single gauss point for the shear stiffness matrix.

In Figure 3, dimensionless central deflections of the simply supported plate on Pasternak foundation are plotted against the total DOFs for h/L=1/50 and increasing foundation shear parameters. It is seen that the midpoint deflections are underestimated due to the shear locking problem when full integration is used in the implementation of R-M PT. It is also observed that the shear locking effect decreases with increasing shear parameter of the foundation. Besides, for dimensionless foundation parameters $k_w'=1$ and $k_p'=1$, very close deflection values are obtained for the Kirchhoff plate solution and R-M plate solution with selective integration even by using (8x8) meshes, Figure 3a. These values attain closer values for $k_w'=1$ and $k_p'=3^4$ and the same values for $k_w'=1$ and $k_p'=5^4$ as seen in Figures 3b and 3c, respectively.

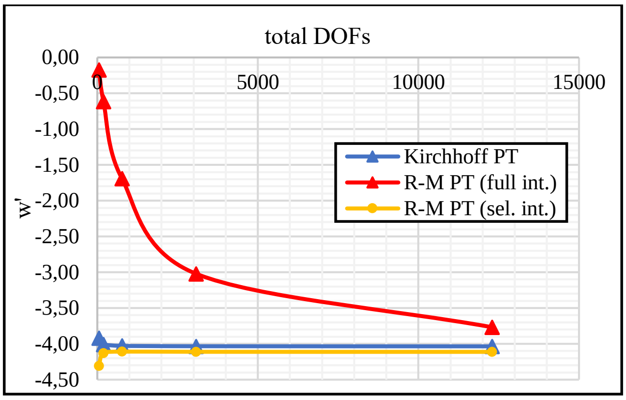


a) $k_w'=1$ $k_p'=1$

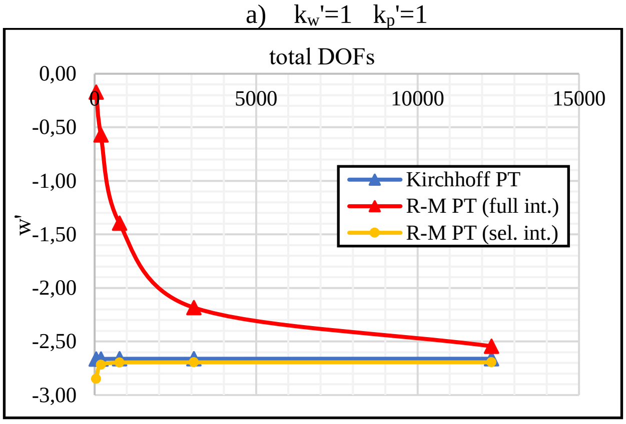


b) $k_w'=1$ $k_p'=3^4$

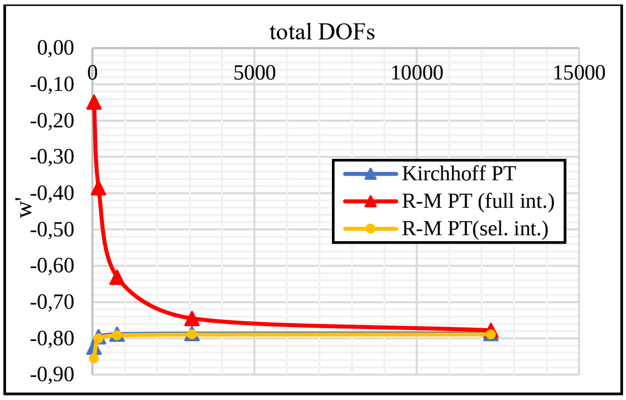


c) $k_w'=1$ $k_p'=5^4$

Figure 3. Dimensionless central deflections (w') of the simply supported square plates on Pasternak foundations for mesh refinement (h/L=1/50)

Then, the thickness to length ratio of the plate is decreased to 1/100. For this case, the shear locking effect is much more pronounced for $k_w'=1$ and $k_p'=1$, Figure 4a. Dimensionless deflections are the same for Kirchhoff plate solution and R-M plate solution with selective integration for all foundation parameters as seen in Figure 4. For $k_w'=1$ and $k_p'=5^4$ foundation parameters, the same deflection values are achieved using the finest mesh when R-M solution with full integration is used, Figure 4c.

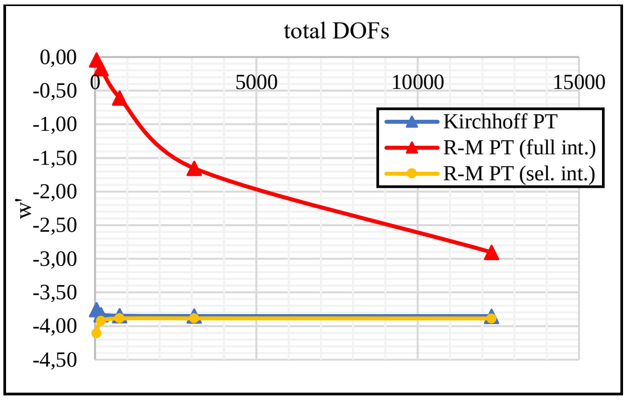


a) $k_w'=1$ $k_p'=1$

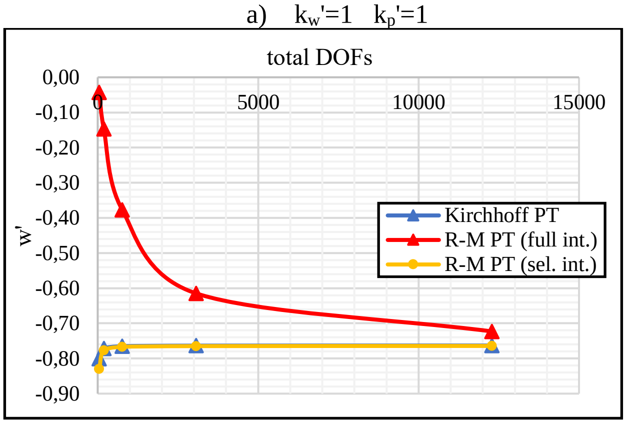


b) $k_w'=1$ $k_p'=3^4$

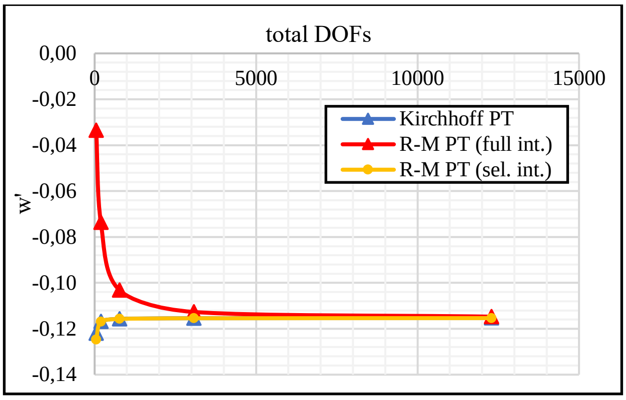


c) $k_w'=1$ $k_p'=5^4$

Figure 4. Dimensionless central deflections (w') of the simply supported square plates on Pasternak foundations for mesh refinement (h/L=1/100)

Computation time is also obtained both for the Kirchhoff PT and R-M PT solutions for successively refined meshes and given comparatively in Table 2.

Table 2. Comparison of computation time between Kirchhoff and R-M (sel. int.) solutions for successively refined meshes

| | Computation time (sec.) | |
|---|---|---|
| | Kirchhoff plate elements | R-M plate elements |
| 4x4 mesh (75 DOFs) | 0.096 | 0.101 |
| 8x8 mesh (243 DOFs) | 0.168 | 0.147 |
| 16x16 mesh (867 DOFs) | 0.38 | 0.462 |
| 32x32 mesh (3267 DOFs) | 1.899 | 1.751 |
| 64x64 mesh (12675 DOFs) | 48.784 | 38.951 |

It is observed that the computation time for both of the solutions are close to each other and the solutions abruptly become computationally expensive in terms of time when using the finest mesh (64x64). Note that the computation time does not significantly change when selective and full integrations are used in the implementation of R-M PT except for the finest mesh. Running time is even longer (51.015 seconds) when full integration is used.

The relative displacement errors of the simply supported square plate on the Pasternak foundation are obtained for the two thickness to length ratios and for different foundation parameters in L2 norm and given comparatively in logarithmic scale as shown in Figures 5-6.

For both of the *h/L* ratios and all foundation parameters, it is observed that the errors are the least when Kirchhoff plate elements are used and the largest when R-M plate elements with full integration are used in the implementation.

For *h/L*=1/50, the relative errors decrease with increasing shear parameter for R-M solution with full integration. The error values do not change for the R-M solution with selective integration and decrease for the Kirchhoff solution when the shear parameter of the foundation is $k_p'=3^4$ as seen in Figure 5.

Then, the relative errors for the plate-foundation system are obtained for *h/L*=1/100 and given in Figure 6. The relative errors decrease when using the R-M plate elements with full integration and do not change for the rest of the solutions except for the Kirchhoff solution for $k_p'=3^4$ where there is a slight decrement in the relative error values.

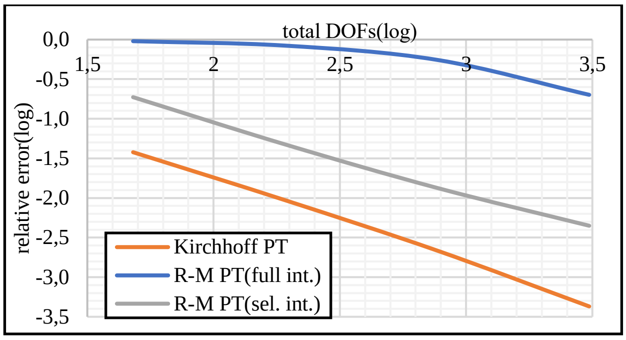


$k_w'=1$ $k_p'=1$

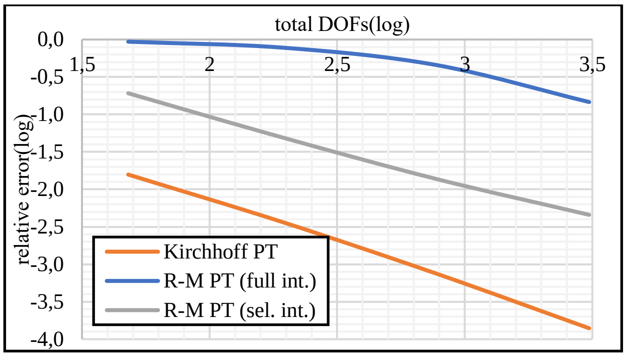


$k_w'=1$ $k_p'=3^4$

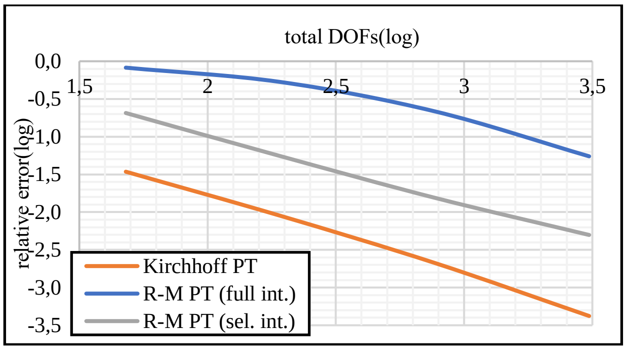


$k_w'=1$ $k_p'=5^4$

Figure 5. Relative errors of the simply supported square plates on Pasternak foundations for mesh refinement (*h/L*=1/50)

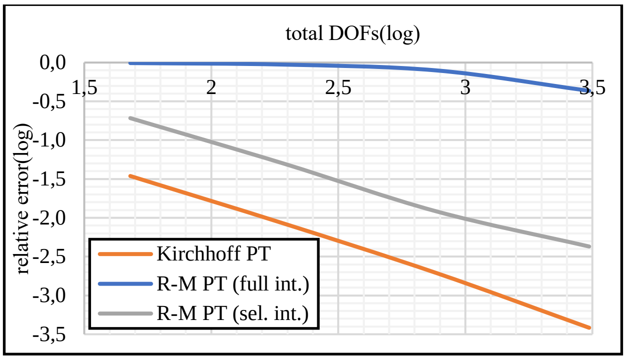


$k_w'=1 \quad k_p'=1$

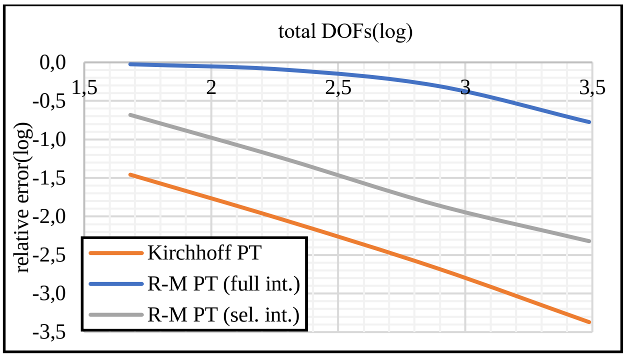


$k_w'=1 \quad k_p'=3^4$

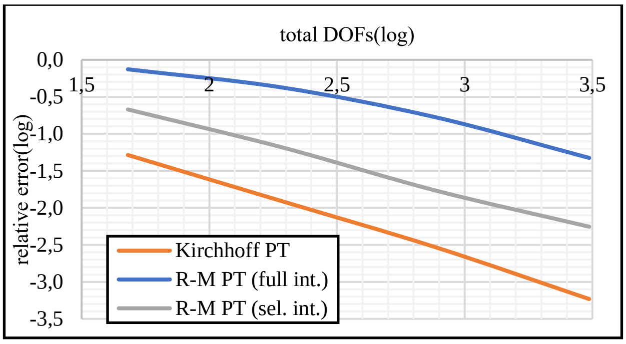


$k_w'=1 \quad k_p'=5^4$

Figure 6. Relative errors of the simply supported square plates on Pasternak foundations for mesh refinement ($h/L$=1/100)

The slopes of relative error-total DOF lines which give the convergence rates of the numerical solutions to the exact solutions are also obtained, Table 3.

For both of the thickness to length ratios, the R-M solutions with full integration have considerably smaller convergence rates which is due to the shear locking effect. The convergences rates decrease as *h/L* ratio decreases from 1/50 to 1/100 and increase as the shear parameter of the foundation increases. The convergence rates for the Kirchhoff solutions are the largest and they almost remain the same for decreasing *h/L* ratio and increasing shear parameter.

Table 3. Convergence rates for the simply supported plate-foundation system

| *h/L* | $k_w'$ | $k_p'$ | Kirchhoff | R-M (full int.) | R-M (sel. int.) |
|---|---|---|---|---|---|
| 1/50 | 1 | 1 | 2.2 | 0.7 | 1.8 |
| | 1 | $3^4$ | 2.3 | 0.9 | 1.8 |
| | 1 | $5^4$ | 2.1 | 1.3 | 1.8 |
| 1/100 | 1 | 1 | 2.2 | 0.4 | 1.8 |
| | 1 | $3^4$ | 2.1 | 0.8 | 1.8 |
| | 1 | $5^4$ | 2.2 | 1.3 | 1.8 |

**Clamped square plate on Pasternak foundation**

The boundary conditions of the same plate-foundation system are converted from simply supported to clamped and the system is solved for the same thickness to length ratios and foundation parameters, Figure 7.

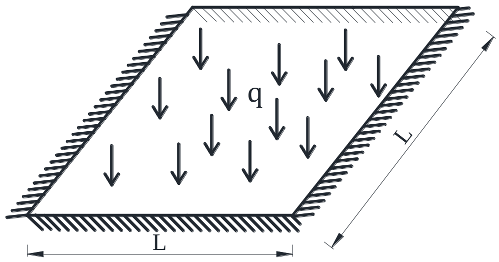


Figure 7. Clamped square plate-foundation system

It is observed from the dimensionless midpoint deflections that the shear locking problem is more effective than the simply supported case for *h/L*=1/50 and this effect is more evident as the thickness to length ratio decreases from 1/50 to 1/100 as seen in Figures 8-9. The dimensionless deflections are the same for the Kirchhoff solution and the R-M solution with selective integration. For the dimensionless foundation parameters $k_w'$=1 and $k_p'$=1, the curves obtained for mesh refinement are steeper for *h/L*=1/100 and there is no tendency to converge to specific values even for the finest mesh, Figure 9a. Closer values are obtained using the R-M elements with full integration as the dimensionless foundation shear parameter increases, Figures 9b-9c.

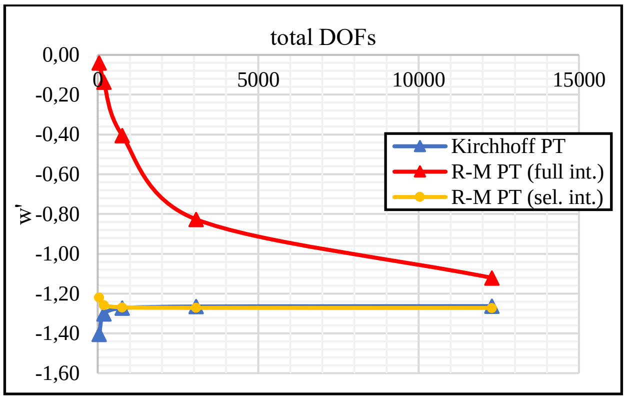


a) $k_w'=1 \quad k_p'=1$

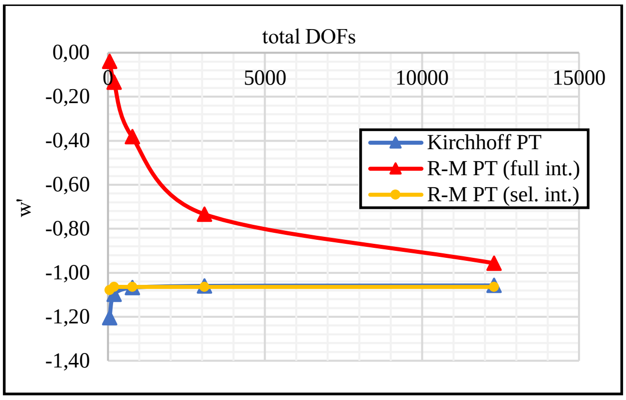


b) $k_w'=1$ $k_p'=3^4$

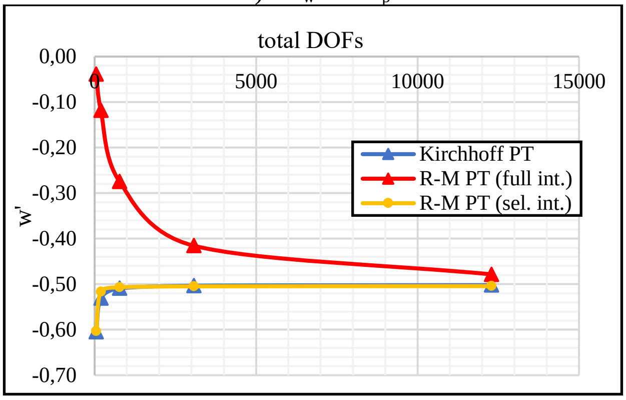


c) $k_w'=1$ $k_p'=5^4$

Figure 8. Dimensionless central deflections (w') of the clamped square plates on Pasternak foundations for mesh refinement (*h/L*=1/50)

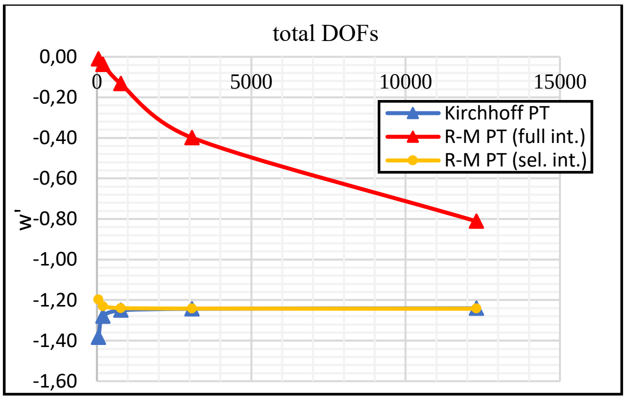


a) $k_w'=1$ $k_p'=1$

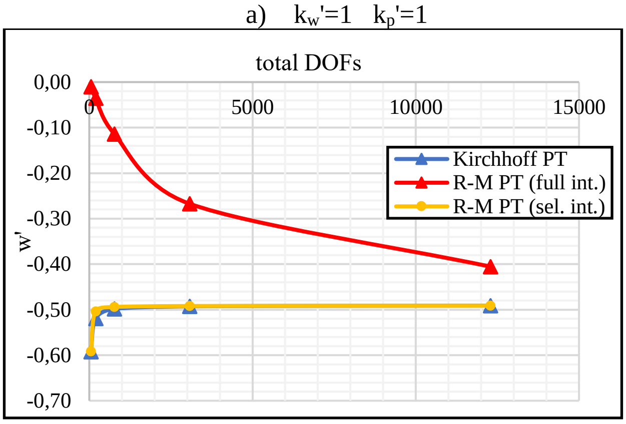


b) $k_w'=1$ $k_p'=3^4$

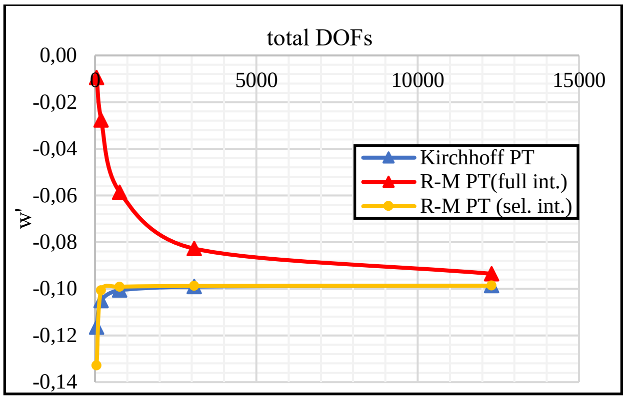


c) $k_w'=1$ $k_p'=5^4$

Figure 9. Dimensionless central deflections (w') of the clamped square plates on Pasternak foundations for mesh refinement (*h/L*=1/100)

The relative errors for the clamped plate-foundation system are given in Figures 10-11. Compared to the simply supported case, the errors obtained using the R-M elements with selective integration are closer to those obtained using the Kirchhoff plate elements. For *h/L*=1/50, the relative errors decrease for $k_p'=5^4$ when R-M elements with full integration is used and increase slightly for the R-M solution with selective integration and the Kirchhoff solution as the shear parameter increases, Figure 10.

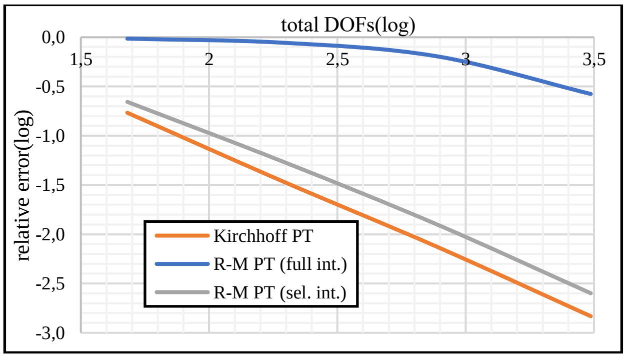


a) $k_w'=1$ $k_p'=1$

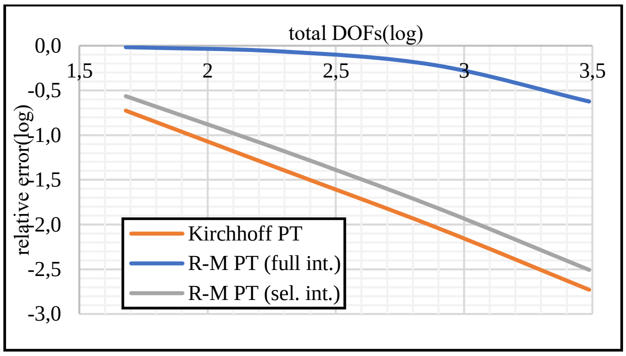


b) $k_w'=1$ $k_p'=3^4$

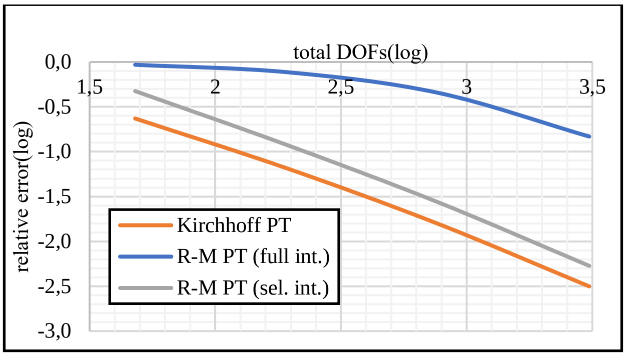


c) $k_w'=1$ $k_p'=5^4$

Figure 10. Relative errors of the clamped square plates on Pasternak foundations for mesh refinement (*h/L*=1/50)

For h/L=1/100, as the shear parameter increases, the relative errors decrease when using the R-M elements with full integration and increase when the R-M elements with selective integration and the Kirchhoff elements are used.

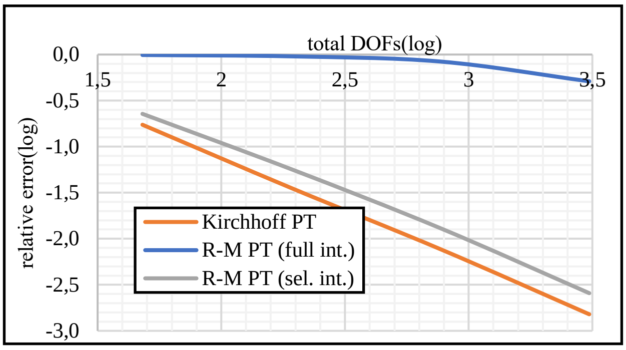


a) $k_w'=1$ $k_p'=1$

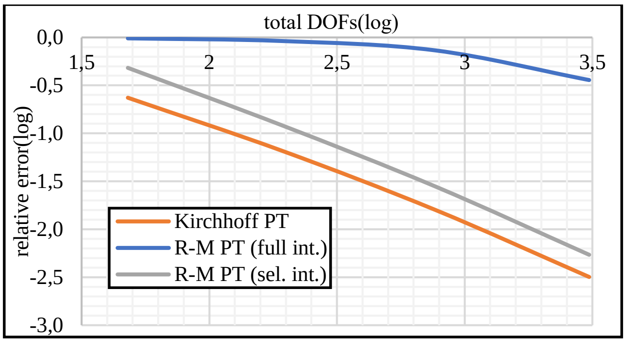


b) $k_w'=1$ $k_p'=3^4$

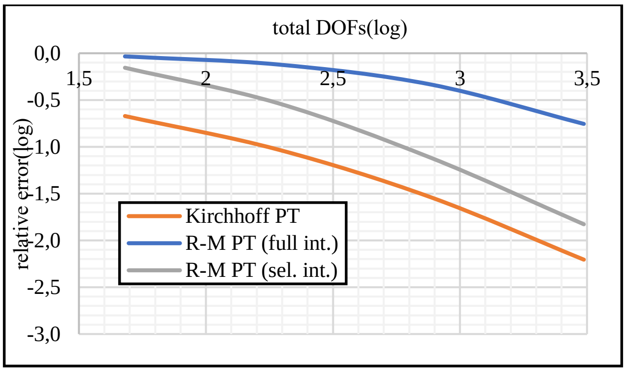


c) $k_w'=1$ $k_p'=5^4$

Figure 11. Relative errors of the clamped square plates on Pasternak foundations for mesh refinement (h/L=1/100)

The convergence rates of the numerical solutions to the exact solutions are given in Table 4 comparatively.

It is observed that the convergence rates for the Kirchhoff solution almost remain the same for decreasing *h/L* ratio and increasing shear parameter except for *h/L*=1/100 and $k_p'=5^4$. When the R-M plate elements with full integration are used, the convergence rates are the smallest. The rates increase for increasing shear parameter and decrease as *h/L* ratio decreases. Using the R-M elements with selective integration, the convergence rates remain the same except for *h/L*=1/100 and $k_p'=5^4$.

Table 4. Convergence rates for the clamped plate-foundation system

| h/L | $k_w'$ | $k_p'$ | Kirchhoff | R-M (full int.) | R-M (sel. int.) |
|---|---|---|---|---|---|
| 1/50 | 1 | 1 | 2.3 | 0.6 | 2.2 |
| | 1 | $3^4$ | 2.2 | 0.7 | 2.2 |
| | 1 | $5^4$ | 2.1 | 0.9 | 2.2 |
| 1/100 | 1 | 1 | 2.3 | 0.3 | 2.2 |
| | 1 | $3^4$ | 2.1 | 0.5 | 2.2 |
| | 1 | $5^4$ | 1.7 | 0.8 | 1.9 |

## Conclusions

In this paper, the finite element analyses of thin plates resting on Pasternak foundations are performed for two thickness to length ratios, two different boundary conditions and three different foundation parameters. The presented Kirchhoff and R-M plate elements are used in the implementation with full and selective integrations and the dimensionless midpoint deflections and the convergence rates due to a uniform loading are obtained and compared with each other.

It is demonstrated that the thin plate-foundation system can easily be modelled by adding the parameter matrices of an existing soil finite element to the respective stiffness matrix terms of both Kirchhoff and R-M plate finite elements.

It is observed that the shear locking effect arises when full integration is used in the implementation of R-M PT and this effect is more evident as the thickness to length ratio of the plate decreases. By using full integration with 2x2 Gauss points for the bending stiffness matrix and selective integration with a single Gauss point for the shear stiffness matrix of the plate element, this problem is alleviated.

Convergence rates do not change significantly for increasing shear parameter of the foundation except for the R-M PT implementation with full integration where the rates increase with increasing shear parameter. Another exception is that the convergence rates for the largest shear parameter for Kirchhoff and R-M (sel.int.) solutions are smaller when the plate-foundation model is clamped.

The convergence rates for R-M solutions with full integration are smaller than the rates for the Kirchhoff and R-M (sel. int.) solutions for both of the boundary conditions and as the thickness of the plate decreases, the rates decrease considerably because of the shear locking effect.

For the Kirchhoff and R-M (sel. int.) solutions, the convergence rates are close to each other for the simply supported plate-foundation system compared to the clamped case.

For the simply supported case, the convergence rates do not change for the Kirchhoff and change slightly for R-M(sel. int.) solutions whereas the convergence rates do not change for both solutions for the clamped plate case as the *h/L* ratio decreases.

Besides, it is observed that although the most converged deflection values are obtained when the finest mesh (64x64) is used in the analyses, it is computationally expensive in terms of time. Using a (32x32) mesh for the Kirchhoff and R-M (sel. int.) solutions would be more suitable since the running time is significantly short and very close results are obtained.

## References


[1] A.E.H. Love, “The small free vibration and deformation of a thin elastic shell”. *Philosophical Transactions of the Royal Society of London A*, vol. 179, pp. 491-546, 1888.

[2] G. Kirchhoff, “Über das Gleichgewicht und die Bewegung einer elastischen Scheibe”, *J. Reine Angew. Math*., vol. 40, pp. 51-88, 1850.

[3] E. Reissner, “The effect of transverse shear deformation on the bending of elastic plates”, *Journal of Applied Mechanics*, vol. 67, pp. A67-A77, 1945.

[4] R.D. Mindlin, “Influence of rotary inertia and shear on flexural motion of isotropic elastic plates”, *Journal of Applied Mechanics*, vol. 18, pp. 31-38, 1951.

[5] Ü.H. Çalık-Karaköse, “Static analysis of thin plates using Kirchhoff and Reissner-Mindlin plate theories”, *The 15th International Scientific Research Congress-Science and Engineering Sciences - (UBAK)*, 17-18 December 2022, Ankara.

[6] E. Winkler, “Theory of Elasticity and Strength of Materials”. *Dominicus, Prague*, 1867.

[7] P.L. Pasternak, “On a new method of analysis of an elastic foundation by means of two foundation constants”. *Cosudarstrennoe Izdatelstvo Literaturi po Stroitelstvu i Arkhitekture, Moscow, USSR*, pp. 1-56, 1954.

[8] C.V.G. Vallabhan, W.T. Straughan, Y.C. Das, “Refined Model of Analysis of Plates of Elastic Foundations”. *Journal of Engineering Mechanics*, vol. 117, no. 12, pp. 2830-2844, 1994.

[9] M. Çelik, and A. Saygun, “A method for the analysis of plates on a two-parameter foundation”, *International Journal of Solids and Structures*, vol. 36, pp. 2891-2915, 1999.

[10] A. Joodaky and I. Joodaky, “A semi-analytical study on static behavior of thin skew plates on Winkler and Pasternak foundations”, *International Journal of Mechanical Sciences,* vol. 100, pp. 322-327, 2015.

[11] Gan, J., Yuan, H., Li, S., Peng, Q., Zhang, H., “A computing method for bending problem of thin plate on Pasternak foundation”, *Advances in Mechanical Engineering*, vol. 12, no. 7, pp. 1-10, 2020.

[12] Y. Xiang, C.M. Wang, S. Kitipornchai, “Exact vibration solution for initially stressed Mindlin plates on Pasternak foundation”. *Int. J. Mech. Sci*., vol. 36, no. 4, pp. 311-316, 1994.

[13] M.H. Omurtag, A. Ozutok, A.Y. Akoz, “Free vibration analysis of Kirchhoff plates resting on elastic foundation by mixed finite element formulation based on Gateaux differential”. *Int. J. Numer. Methods Eng.*, vol. 40, no. 2, pp. 295-317, 1997.

[14] D. Zhou, Y.K. Cheung, S.H. Lo, F.T.K. Au, “Three-dimensional vibration analysis of rectangular thick plates on Pasternak foundations”. *Int. J. Numer. Methods. Eng.*, vol. 59, no. 10, pp. 1313-1334, 2004.

[15] MATLAB R2019a, Natick, Massachusetts: The Mathworks, Inc.

[16] R.J. Melosh, “Structural analysis of solids”. *J. Structural Engineering*, ASCE, vol. 4, pp. 205-223, 1963.

[17] O.C. Zienkiewicz, and Y.K. Cheung, “The finite element method for analysis of elastic isotropic and isotropic slabs”. *Proc. Inst. Civ. Engng*., vol. 28, pp. 471-88, 1964.

[18] O.C. Zienkiewicz, and Y.K. Cheung, “Finite element procedures in the solution of plate and shell problems in Stress Analysis”, *O.C. Zienkiewicz and G.S. Holister (Eds.), Chapter 8. John Wiley & Sons, Chichester*, 1965.

[19] T.J.R. Hughes, R.L. Taylor, and W. Kanok-Nukulchai, “A simple and efficient finite element for plate bending”, *Int. J. Numer. Meth. Engng*., vol. 11, pp. 1529-43, 1977.

[20] E.D.L. Pugh, E. Hinton, and O.C. Zienkiewicz, “A study of quadrilateral plate bending elements with reduced integration”. *J. Appl. Mech*., vol. 12, pp. 1059-1079, 1978.

[21] Ü.H. Çalık-Karaköse, “Influence Surface Coefficients of Plates Resting on Pasternak Foundation”, *DUJE (Dicle University Journal of Engineering),* vol. 13, no. 2, pp. 371-377, 2022.

[22] K.Y. Lam, C.M. Wang, X.Q. He, “Canonical exact solution for Levy-plates on two-parameter foundation using Green’s functions”. *Eng. Struct*., vol. 22, no. 4, pp. 364-378, 2000.